

## 1. TENSORIAL ASPECTS OF PHYSICAL PROPERTIES

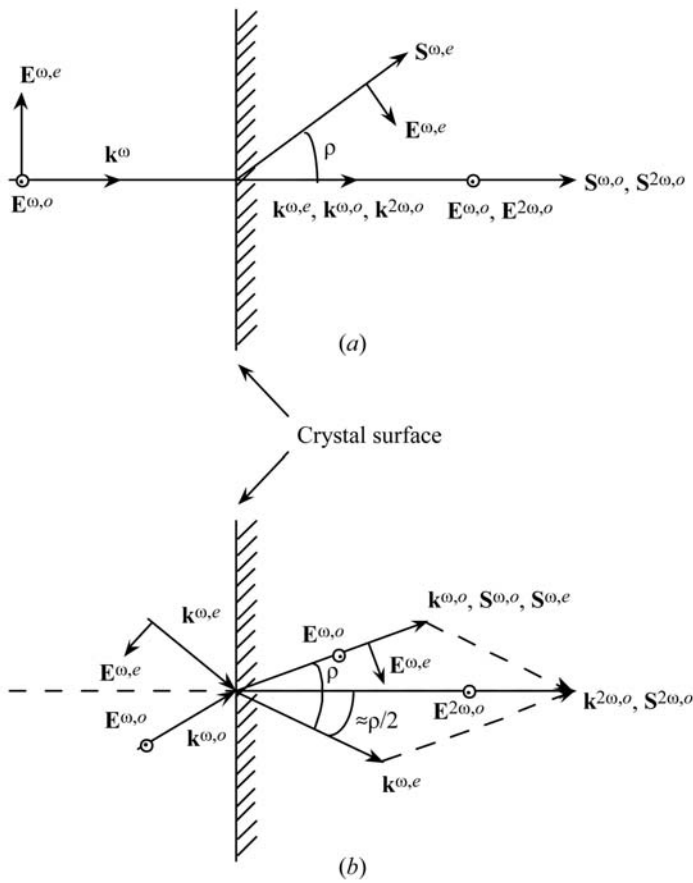


Fig. 1.7.3.11. Comparison between (a) collinear and (b) special non-collinear phase matching for (o eo) type-II SHG.  $\mathbf{k}^{\omega,o}$ ,  $\mathbf{k}^{\omega,e}$  and  $\mathbf{k}^{2\omega,o}$  are the wavevectors,  $\mathbf{S}^{\omega,o}$ ,  $\mathbf{S}^{\omega,e}$  and  $\mathbf{S}^{2\omega,o}$  are the Poynting vectors of the fundamental and harmonic waves, and  $\mathbf{E}^{\omega,o}$ ,  $\mathbf{E}^{\omega,e}$  and  $\mathbf{E}^{2\omega,o}$  are the electric field vectors;  $\rho$  is the walk-off angle in the collinear case and the angle between  $\mathbf{k}^{\omega,o}$  and  $\mathbf{k}^{\omega,e}$  inside the crystal for the non-collinear interaction.

because the saturation phenomenon of type-II CPM is avoided.

(iv) *Effect of temporal walk-off.*

Even if the SHG is phase matched, the fundamental and harmonic group velocities,  $v_g(\omega) = \partial\omega/\partial k$ , are generally mismatched. This has no effect with continuous wave (c.w.) lasers. For pulsed beams, the temporal separation of the different beams during the propagation can lead to a decrease of the temporal overlap of the pulses. Indeed, this walk-off in the time domain affects the conversion efficiency when the pulse separations are close to the pulse durations. Then after a certain distance,  $L_\tau$ , the pulses are completely separated, which entails a saturation of the conversion efficiency, for both types I and II (Tomov *et al.*, 1982). Three group velocities must be considered for type II. Type I is simpler, because the two fundamental waves have the same velocity, so  $L_\tau = \tau/[v_g^{-1}(\omega) - v_g^{-1}(2\omega)]$ , which defines the optimum crystal length, where  $\tau$  is the pulse duration. For type-I SHG of 532 nm in  $\text{KH}_2\text{PO}_4$  (KDP),  $v_g(266 \text{ nm}) = 1.84 \times 10^8 \text{ m s}^{-1}$  and  $v_g(532 \text{ nm}) = 1.94 \times 10^8 \text{ m s}^{-1}$ , so  $L_\tau = 3.5 \text{ mm}$  for 1 ps. For the usual nonlinear crystals, the temporal walk-off must be taken into account for pico- and femtosecond pulses.

1.7.3.3.2.2. *Non-resonant SHG with undepleted pump and transverse and longitudinal Gaussian beams*

We now consider the general situation where the crystal length can be larger than the Rayleigh length.

The Gaussian electric field amplitudes of the two eigen electric field vectors inside the nonlinear crystal are given by

$$E^\pm(X, Y, Z) = E_o^\pm \frac{w_o}{w(Z)} \exp \left[ -\frac{(X + \rho^+ Z)^2 + (Y + \rho^- Z)^2}{w^2(Z)} \right] \times \exp \left( i \left\{ k^\pm Z - \arctan(Z/z_R) + \frac{k^\pm [(X + \rho^+ Z)^2 + (Y + \rho^- Z)^2]}{2Z[1 + (z_R^2/Z^2)]} \right\} \right) \quad (1.7.3.55)$$

with  $\rho^- = 0$  for  $E^+$  and  $\rho^+ = 0$  for  $E^-$ .

$(X, Y, Z)$  is the wave frame defined in Fig. 1.7.3.1.  $E_o^\pm$  is the scalar complex amplitude at  $(X, Y, Z) = (0, 0, 0)$  in the vibration planes  $\Pi^\pm$ .

We consider the refracted waves  $E^+$  and  $E^-$  to have the same longitudinal profile inside the crystal. Then the  $(1/e^2)$  beam radius is given by  $w(Z) = w_o^2[1 + (Z^2/z_R^2)]$ , where  $w_o$  is the minimum beam radius located at  $Z = 0$  and  $z_R = kw_o^2/2$ , with  $k = (k^+ + k^-)/2$ ;  $z_R$  is the Rayleigh length, the length over which the beam radius remains essentially collimated;  $k^\pm$  are the wavevectors at the wavelength  $\lambda$  in the direction of propagation  $Z$ . The far-field half divergence angle is  $\Delta\alpha = 2/kw_o$ .

The coordinate systems of (1.7.3.22) are identical to those of the parallel-beam limit defined in (iii).

In these conditions and by assuming the undepleted pump approximation, the integration of (1.7.3.22) over  $(X, Y, Z)$  leads to the following expression of the power conversion efficiency (Zondy, 1991):

$$\eta_{\text{SHG}}(L) = \frac{P^{2\omega}(L)}{P^\omega(0)} = CLP^\omega(0) \frac{h(L, w_o, \rho, f, \Delta k)}{\cos^2 \rho_{2\omega}}$$

with

$$C = 5.95 \times 10^{-2} \frac{2N - 1}{N} \frac{d_{\text{eff}}^2}{\lambda_\omega^3} \frac{n_1^\omega + n_2^\omega}{2} \frac{T_3^{2\omega} T_1^\omega T_2^\omega}{n_3^{2\omega} n_1^\omega n_2^\omega} \quad (\text{W}^{-1} \text{ m}^{-1}) \quad (1.7.3.56)$$

in the same units as equation (1.7.3.42).

For type I,  $n_1^\omega = n_2^\omega$ ,  $T_1^\omega = T_2^\omega$ , and for type II  $n_1^\omega \neq n_2^\omega$ ,  $T_1^\omega \neq T_2^\omega$ .

The attenuation coefficient is written

$$h(L, w_o, \rho, f, \Delta k) = [2z_R(\pi)^{1/2}/L] \int_{-\infty}^{+\infty} |H(a)|^2 \exp(-4a^2) da$$

with

$$H(a) = \frac{1}{(2\pi)^{1/2}} \int_{-fL/z_R}^{L(1-f)/z_R} \frac{d\tau}{1 + i\tau} \exp \left[ -\gamma^2 \left( \tau + \frac{fL}{z_R} \right)^2 - i\sigma\tau \right]$$

$$\text{for type I: } \gamma = 0 \text{ and } \sigma = \Delta k z_R + 4 \frac{\rho z_R}{w_o} a$$

$$\text{for type II: } \gamma = \frac{\rho z_R}{w_o(2)^{1/2}} \text{ and } \sigma = \Delta k z_R + 2 \frac{\rho z_R}{w_o} a,$$

$$(1.7.3.57)$$

where  $f$  gives the position of the beam waist inside the crystal:  $f = 0$  at the entrance and  $f = 1$  at the exit surface. The definition and approximations relative to  $\rho$  are the same as those discussed for the parallel-beam limit.  $\Delta k$  is the mismatch parameter, which takes into account first a possible shift of the pump beam direction from the collinear phase-matching direction and secondly the distribution of mismatch, including collinear and non-collinear interactions, due to the divergence of the beam, even if the beam axis is phase-matched.

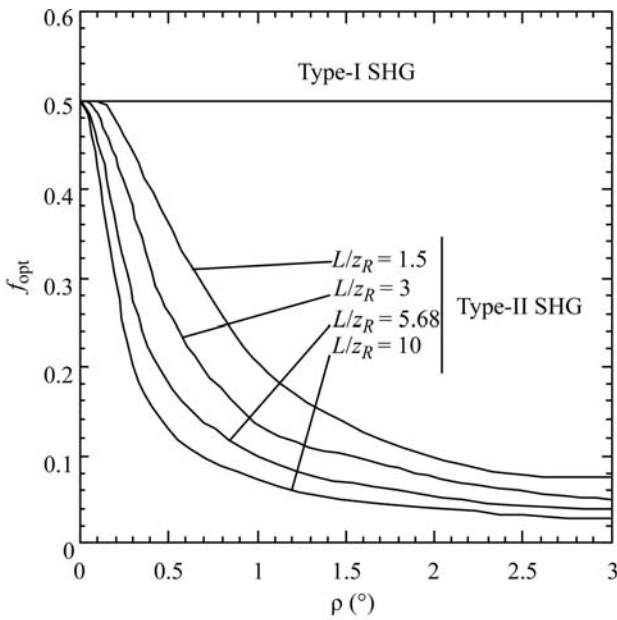


Fig. 1.7.3.12. Position  $f_{\text{opt}}$  of the beam waist for different values of walk-off angles and  $L/z_R$ , leading to an optimum SHG conversion efficiency. The value  $f_{\text{opt}} = 0.5$  corresponds to the middle of the crystal and  $f_{\text{opt}} = 0$  corresponds to the entrance surface (Fève & Zondy, 1996).

The computation of  $h(L, w_o, \rho, f, \Delta k)$  allows an optimization of the SHG conversion efficiency which takes into account  $L/z_R$ , the waist location  $f$  inside the crystal and the phase mismatch  $\Delta k$ .

Fig. 1.7.3.12 shows the calculated waist location which allows an optimal SHG conversion efficiency for types I and II with optimum phase matching. From Fig. 1.7.3.12, it appears that the optimum waist location for type I, which leads to an optimum conversion efficiency, is exactly at the centre of the crystal,  $f_{\text{opt}} = 0.5$ . For type II, the focusing ( $L/z_R$ ) is stronger and the walk-off angle is larger, and the optimum waist location is nearer the entrance of the crystal. These facts can be physically understood: for type I, there is no walk-off for the fundamental beam, so the whole crystal length is efficient and the symmetrical configuration is obviously the best one; for type II, the two fundamental rays can be completely separated in the waist area, which has the strongest intensity, when the waist location is far from the entrance face; for a waist location nearer the entrance, the waist area can be selected and the enlargement of the beams from this area allows a spatial overlap up to the exit face, which leads to a higher conversion efficiency.

The divergence of the pump beam imposes non-collinear interactions such that it could be necessary to shift the direction of propagation of the beam from the collinear phase-matching direction in order to optimize the conversion efficiency. This leads to the definition of an optimum phase-mismatch parameter  $\Delta k_{\text{opt}} (\neq 0)$  for a given  $L/z_R$  and a fixed position of the beam waist  $f$  inside the crystal.

The function  $h(L, w_o, \rho, f_{\text{opt}}, \Delta k_{\text{opt}})$ , written  $h_m(B, L)$ , is plotted in Fig. 1.7.3.13 as a function of  $L/z_R$  for different values of the walk-off parameter, defined as  $B = (1/2)\rho\{(k_o^\omega + k_e^\omega)/2\}L^{1/2}$ , at the optimal waist location and phase mismatch.

Consider first the case of angular NCPM ( $B = 0$ ) where type-I and -II conversion efficiencies obviously have the same  $L/z_R$  evolutions. An optimum focusing at  $L/z_R = 5.68$  exists which defines the optimum focusing  $z_{R_{\text{opt}}}$  for a given crystal length or the optimal length  $L_{\text{opt}}$  for a given focusing. The conversion efficiency decreases for  $L/z_R > 5.68$  because the increase of the ‘average’ beam radius over the crystal length due to the strong focusing becomes more significant than the increased peak power in the waist area.

In the case of angular CPM ( $B \neq 0$ ), the  $L/z_R$  variation of type-I conversion efficiency is different from that of type II. For

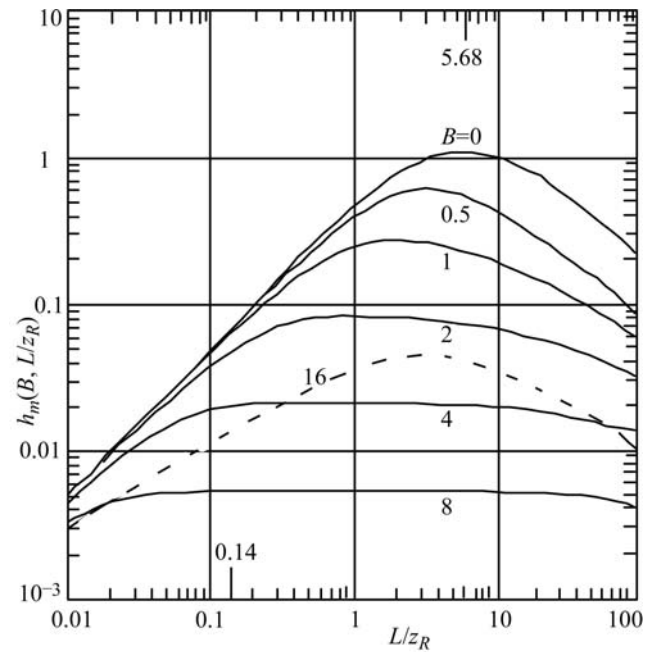


Fig. 1.7.3.13. Optimum walk-off function  $h_m(B, L)$  as a function of  $L/z_R$  for various values of  $B = (1/2)\rho\{(k_o^\omega + k_e^\omega)/2\}L^{1/2}$ . The curve at  $B = 0$  is the same for both type-I and type-II phase matching. The full lines at  $B \neq 0$  are for type II and the dashed line at  $B = 16$  is for type I. (From Zondy, 1990).

type I, as  $B$  increases, the efficiency curves keep the same shape, with their maxima abscissa shifting from  $L/z_R = 5.68$  ( $B = 0$ ) to  $2.98$  ( $B = 16$ ) as the corresponding amplitudes decrease. For type II, an optimum focusing becomes less and less apparent, while  $(L/z_R)_{\text{opt}}$  shifts to much smaller values than for type I for the same variation of  $B$ ; the decrease of the maximum amplitude is stronger in the case of type II. The calculation of the conversion efficiency as a function of the crystal length  $L$  at a fixed  $z_R$  shows a saturation for type II, in contrast to type I. The saturation occurs at  $B \simeq 3$  with a corresponding focusing parameter  $L/z_R \simeq 0.4$ , which is the limit of validity of the parallel-beam approximation. These results show that weak focusing is suitable for type II, whereas type I allows higher focusing.

The curves of Fig. 1.7.3.14 give a clear illustration of the walk-off effect in several usual situations of crystal length, walk-off angle and Gaussian laser beam. The SHG conversion efficiency is calculated from formula (1.7.3.56) and from the function (1.7.3.57) at  $f_{\text{opt}}$  and  $\Delta k_{\text{opt}}$ .

#### 1.7.3.3.2.3. Non-resonant SHG with depleted pump in the parallel-beam limit

The analytical integration of the three coupled equations (1.7.3.22) with depletion of the pump and phase mismatch has only been done in the parallel-beam limit and by neglecting the walk-off effect (Armstrong *et al.*, 1962; Eckardt & Reintjes, 1984; Eimerl, 1987; Milton, 1992). In this case, the three coordinate systems of equations (1.7.3.22) are identical,  $(X, Y, Z)$ , and the general solution may be written in terms of the Jacobian elliptic function  $\text{sn}(m, \alpha)$ .

For the simple case of type I, *i.e.*  $E_1^\omega(X, Y, Z) = E_2^\omega(X, Y, Z) = E^\omega(X, Y, Z) = E_{\text{tot}}^\omega(X, Y, Z)/(2^{1/2})$ , the exit second harmonic intensity generated over a length  $L$  is given by (Eckardt & Reintjes, 1984)

$$I^{2\omega}(X, Y, L) = I_{\text{tot}}^\omega(X, Y, 0) T^{2\omega} T^\omega v_b^2 \text{sn}^2 \left[ \frac{\Gamma(X, Y)L}{v_b}, v_b^4 \right]. \quad (1.7.3.58)$$